Supporting Information

Green-Emitting Powders of Zero-Dimensional Cs_4PbBr_6: Delineating the Intricacies of the Synthesis and the Origin of Photoluminescence

Aniruddha Ray,[†,‡] Daniela Maggioni,[∥] Dmitry Baranov,[†] Zhiya Dang,[†] Mirko Prato,[Δ] Quinten A. Akkerman,[†] Luca Goldoni,[⊥] Enrico Caneva,[∥] Liberato Manna,*,[†] Ahmed L. Abdelhady*,[†]

[†]Nanochemistry Department, [Δ]Materials Characterization Facility, and [⊥]Analytical Chemistry Lab, Istituto Italiano di Tecnologia, Via Morego 30, 16163 Genova, Italy

[‡]Dipartimento di Chimica e Chimica Industriale, Università degli Studi di Genova, Via Dodecaneso, 31, 16146, Genova, Italy

[∥]Dipartimento di Chimica, and [§]UNITECH COSPECT (COmprehensive Substances characterization via advanced sPECTtrometry), Università degli Studi di Milano, Via Golgi 19, 20133 Milano, Italy

Corresponding Author
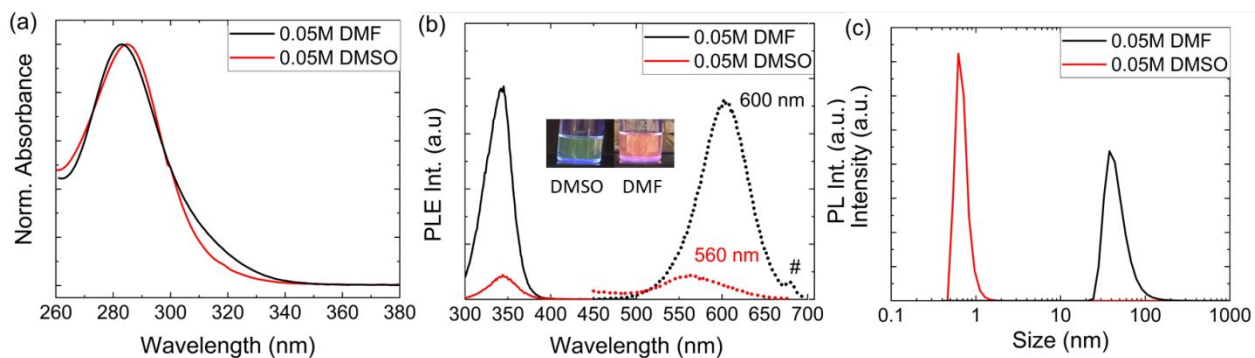
*liberato.manna@iit.it, ahmed.abdelhady@iit.it

Figure S1. (a) Absorbance spectra, (b) PLE (solid lines) and PL (dotted lines) spectra of 0.05 M

$PbBr_2$ in DMSO and DMF (# = the small peak at 670 nm is the second order Rayleigh peak due to

excitation at 335 nm). Inset in (b): picture of both solutions under UV-lamp. (c) Corresponding

DLS analysis.

To gain a deeper understanding on the formation of the lead polybromide species we also studied
the absorbance, PLE, and PL of both solutions in the absence of CsBr (0.05 M $PbBr_2$ in DMSO
and in DMF) and the spectra are shown in Figure S1. The DMF solution showed slightly increased
absorbance near 310 nm compared to the DMSO solution (Figure S1a). Under the UV-lamp, the
DMSO and DMF solutions showed green and orange emission, inset in Figure S1b, and their PL
peaks were recorded at 560 and 600 nm, respectively (Figure S1b). Hence, in the absence of CsBr,
$[PbBr_4]^{2-}$ is already formed in the DMSO solution, while only $[PbBr_3]^-$ is detected in the DMF
solution. Importantly, the DLS measurements, shown in Figure S1c, once again revealed that the
solvodynamic size of the lead bromide species is up to an order of magnitude larger in DMF
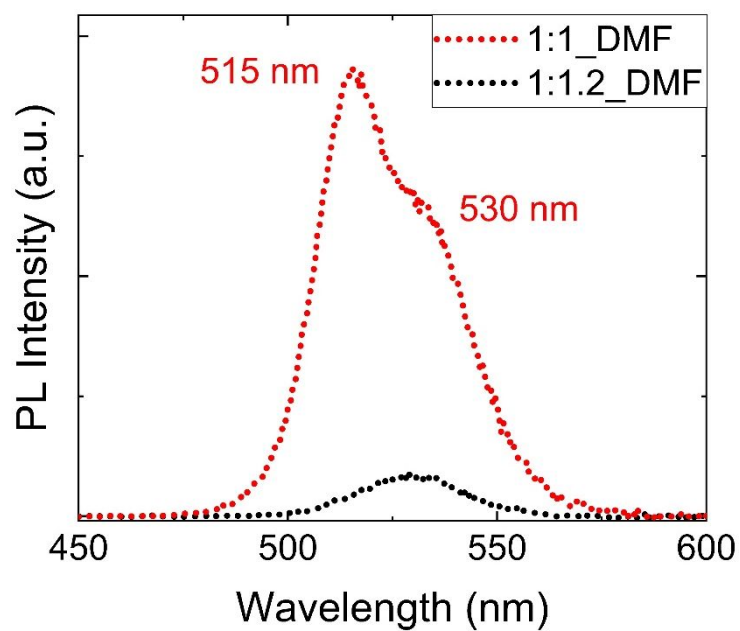compared to the ones formed in DMSO.

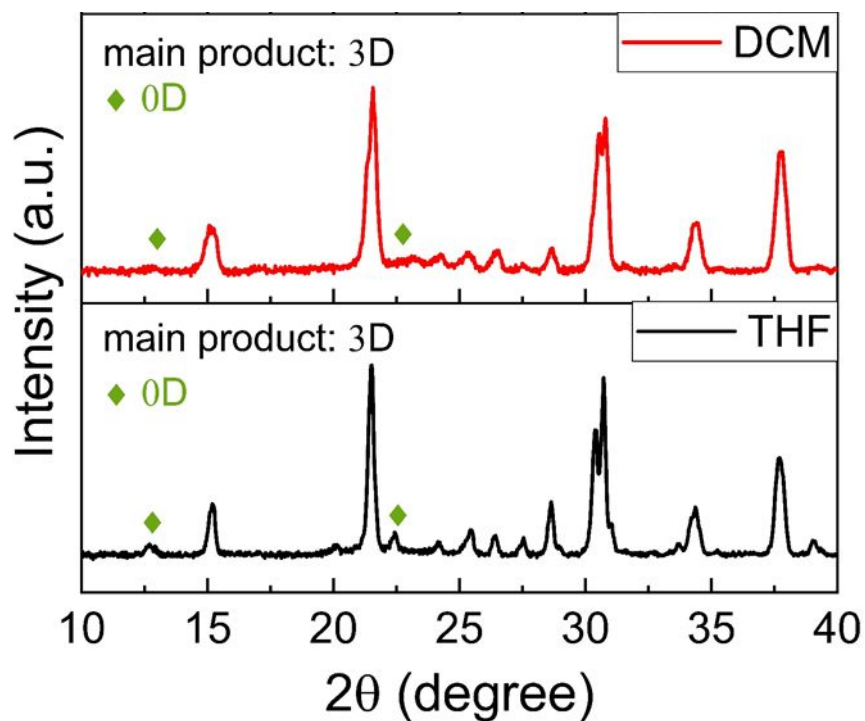**Figure S2.** PL of 3D CsPbBr$_3$ powders obtained from varying ratios of CsBr:PbBr$_2$ in DMF.

Figure S3. XRD patterns of powders precipitated from a 1:1 CsBr:PbBr$_2$ mixture dissolved in a mixed solvent of 1:1 DMSO:DMF.
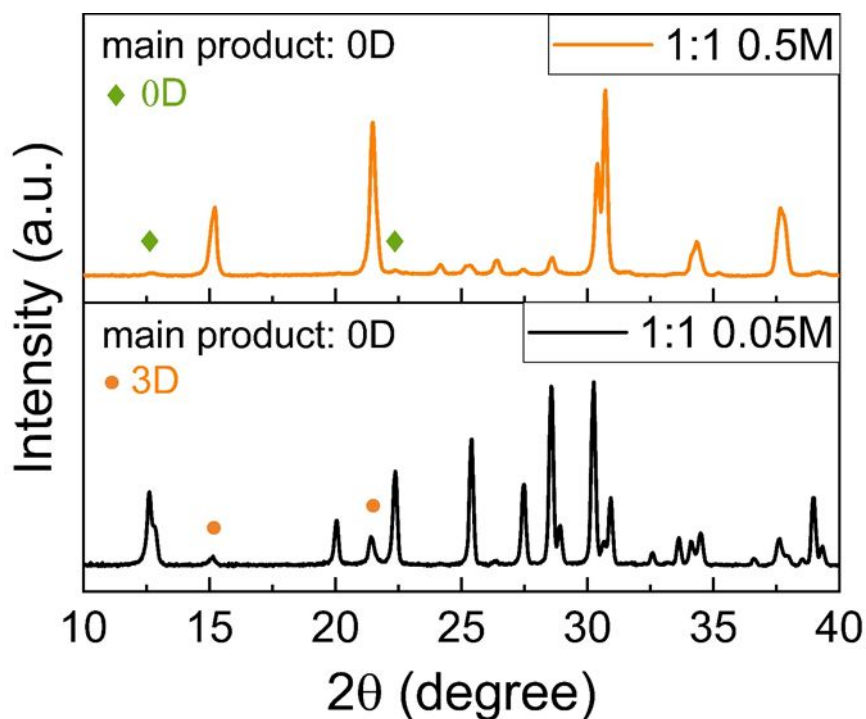

Figure S4. XRD patterns of powders precipitated from a 0.05 M and a 0.5 M 1:1 CsBr:PbBr$_2$ precursor solutions in DMSO.
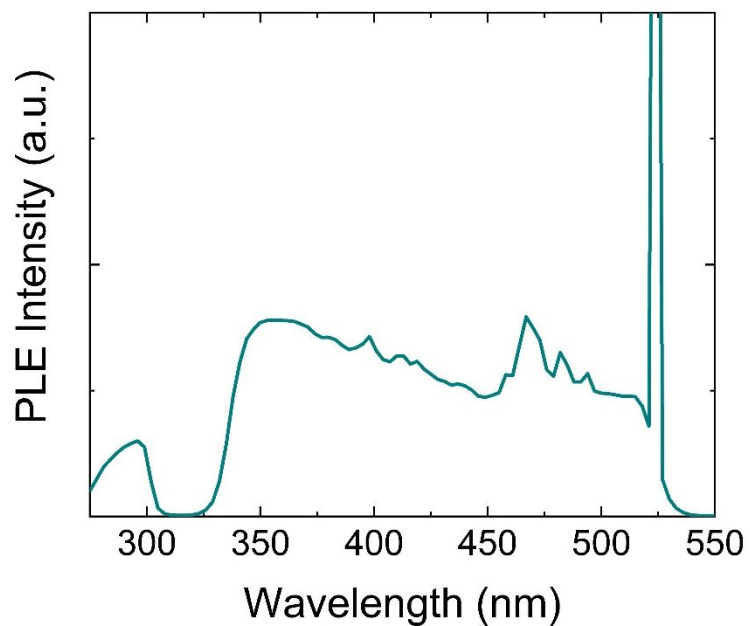
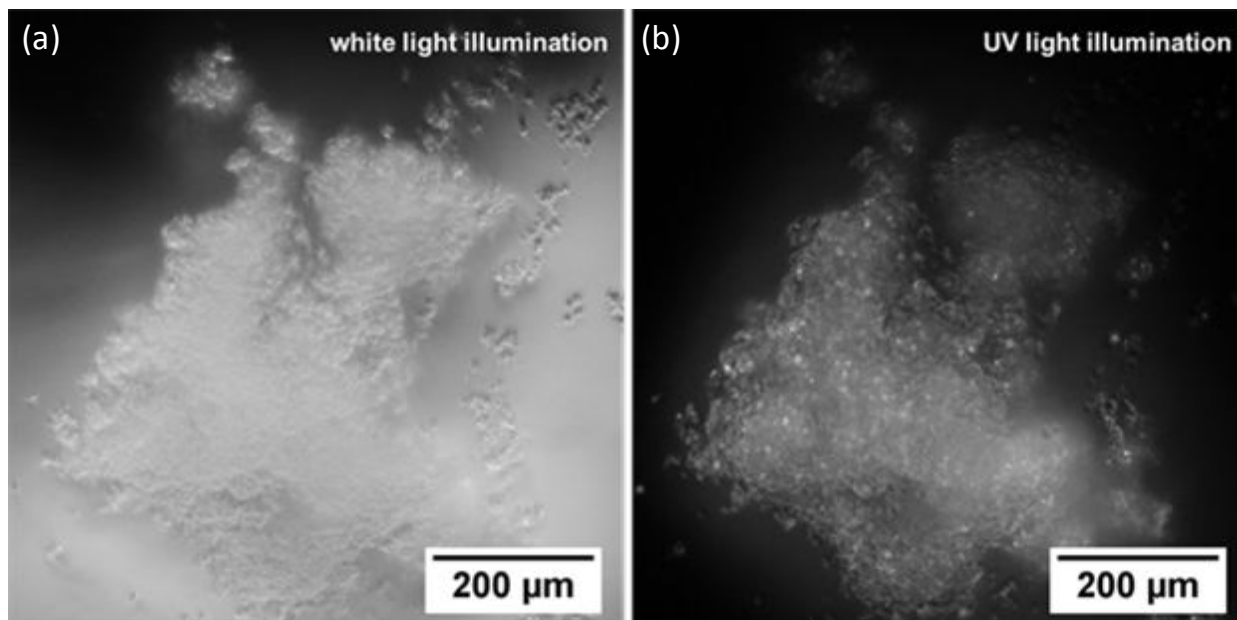**Figure S5.** PLE spectra of 4:1_DMSO powder tracking emission at 520 nm.

Figure S6. Optical images of the 4:1_DMSO powder under (a) white light illumination and (b) UV light.
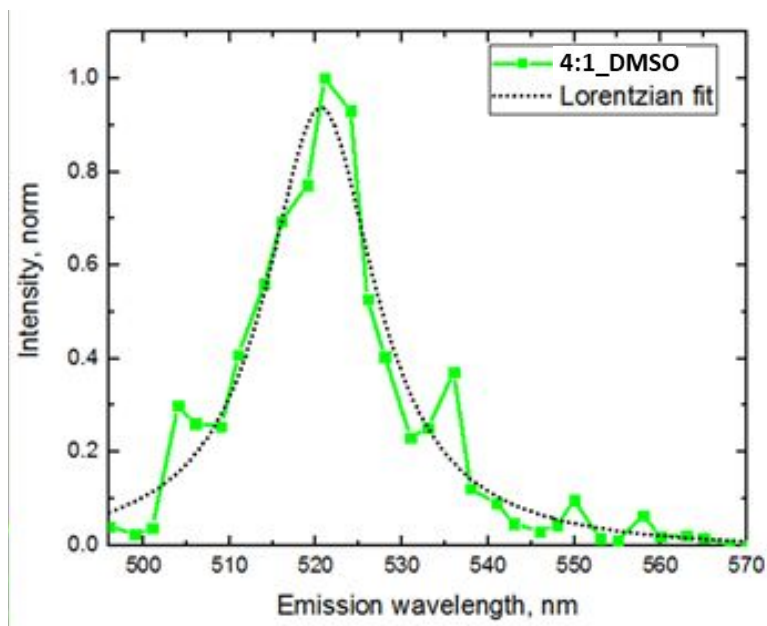
Figure S7. PL spectra of the 4:1_DMSO powder obtained from confocal image and its Lorentzian fit (λmax = 520.6 nm).
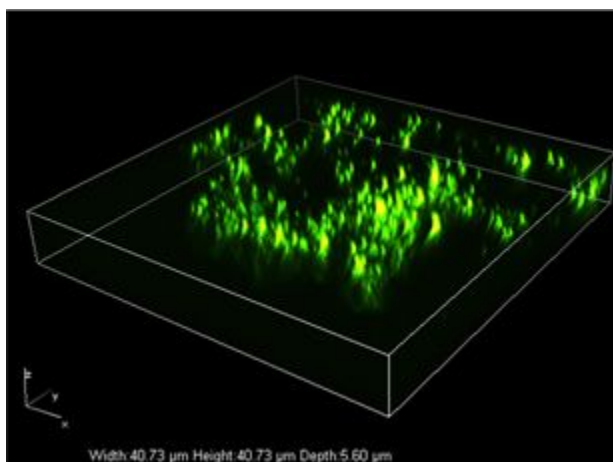

Figure S8. Confocal PL microscopy volume view of the 4:1_DMSO powder showing distribution of bright spots in space.
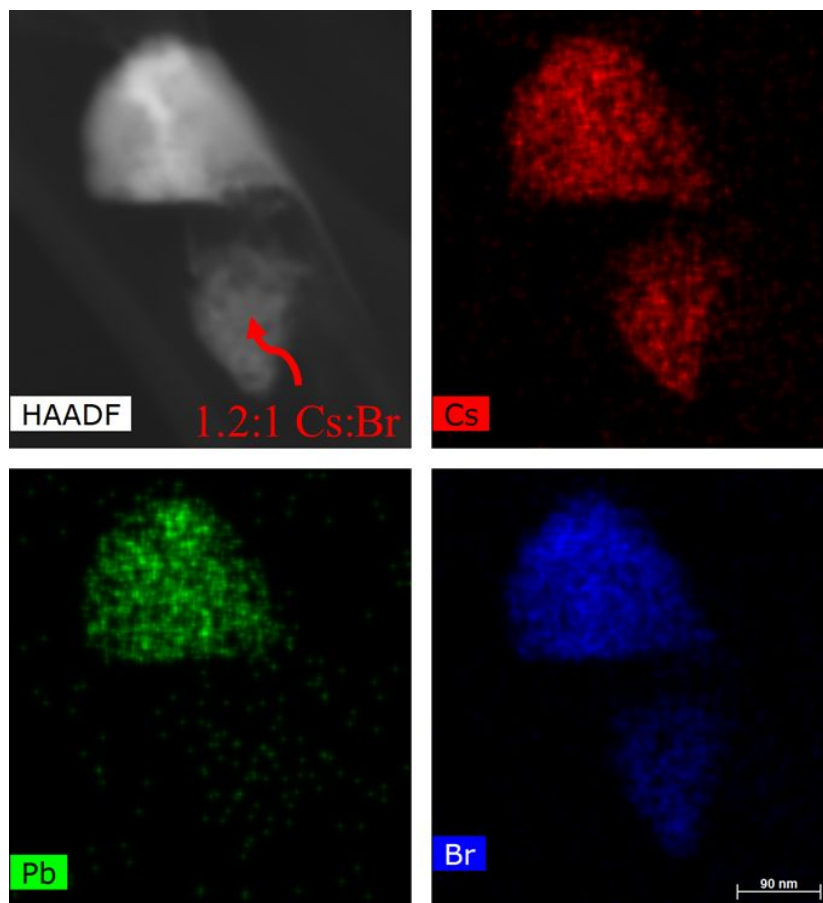
Figure S9. High-angle annular dark-field (HAADF) and elemental analysis of the 4:1_DMSO sample showing Cs_4PbBr_6 and CsBr particles are individual entities.

Table S1. Elemental composition of 4:1_DMSO sample obtained using XPS and EDS.

Technique	Stoichiometry
XPS	$Cs_{4.17}PbBr_{5.27}$
EDS	$Cs_{4.25}PbBr_{5.36}$

Note S1:

The ratio of the 3D impurity in the 0D powder was calculated from XRD following the RIR (reference intensity ratio) method.

$$\frac{I_{0D}}{I_{3D}} = \frac{(RIR)_{0D}}{(RIR)_{3D}} \frac{X_{0D}}{X_{3D}}$$

I_{0D} – Integrated area of selected 0D peak
I_{3D} – Integrated area of selected 3D peak
$(RIR)_{0D}$ – Reference intensity ratio of trigonal 0D

$(RIR)_{3D}$ – Reference intensity ratio of orthorhombic 3D
X_{0D} – Weight fraction of hexagonal 0D
X_{3D} – Weight fraction of hexagonal 0D